Sustainable Energy & Fuels

ROYAL SOCIETY OF CHEMISTRY

PAPER

View Article Online
View Journal | View Issue

Cite this: *Sustainable Energy Fuels*, 2021, **5**, 449

Carbon dots for photocatalytic H_2 production in aqueous media with molecular Co catalysts†

Kalliopi Ladomenou, * Georgios Landrou, Georgios Charalambidis,* Emmanouil Nikoloudakis and Athanassios G. Coutsolelos *

Received 2nd November 2020
Accepted 15th November 2020

DOI: 10.1039/d0se01630f

rsc.li/sustainable-energy

Carbon dots and nitrogen doped carbon dots were effectively synthesized and characterized. Their use as light harvesters was examined in the presence of three different cobalt-based catalysts and tris(carboxyethyl)phosphine/ascorbic acid (TCEP/Asc), as the sacrificial electron donor (SED). The electrons are transferred from the valence band (VB) to the conduction band (CB) of the carbon dots and the holes that are formed are filled by electrons transferred from the SED. The best photocatalytic system reported herein produces 17.1 μmol of H_2 (TON_{CAT} = 859) under UV radiation for 52 h. The same system can produce 5.3 μmol of H_2 (TON_{CAT} = 264) under the Cretan sun for 21 days of solar irradiation.

Introduction

Even though hydrogen is the most abundant element on Earth, it is present in chemical compounds and needs to be extracted with the consumption of energy, in order to use it as a fuel. Therefore, it is of great importance to produce and store H_2 using alternative and economically feasible methods in order to replace fossil fuels.[1] Hydrogen is believed to have high density, and to be a clean and environmentally friendly energy source, since upon its combustion it produces no pollutants. Therefore, H_2 is an attractive solution to resolve the global energy and environmental problems.[2,3] Many studies are based on efficient H_2 production from which one of the most promising is the photocatalytic splitting of water.[4,5] In order to produce an efficient photocatalytic system, three main components must be combined and operated together: a molecule or a material able to absorb the energy of light (light harvester), a catalyst, and a sacrificial electron donor.[6] The photosensitizer absorbs light and produce electrons and hole pairs, then it promotes charge transfer to the catalyst that stimulates the reduction of protons. Finally, the sacrificial electron donor fuels the photosensitizer with electrons in order to start the second catalytic cycle. For an efficient photocatalytic system, it is crucial to use a light absorber that is stable, absorbs light in a broad light region, exhibits long lifetimes for effective charge separation, is easily prepared with low-cost and contains noble-metal free elements. Moreover, the redox potentials of the photosensitizer and the catalyst must be well complemented so that the charge transfer process will be thermodynamically and kinetically favored. For that purpose, much research has been done towards the synthesis of numerous light harvesting organic or inorganic molecules and nanomaterials.[7–11] The molecular dyes appear to have some disadvantages such as they suffer from photostability in water and their preparation often requires demanding synthetic procedures. On the other hand, among the plethora of nanomaterials, carbon dots exhibit several advantages compared to semiconductor materials that appear to often have toxic metals in their structure.[9,12–14] Carbon dots are small carbon nanoparticles with usual size less than 10 nm. The surface of these materials can be passivated with several elements such as nitrogen in order to modify their fluorescence properties and to facilitate charge separation due to the coexistence of p- and n-domains. Moreover, carbon dots appear to have distinctive donor/acceptor properties, exceptional electron transfer characteristics, photostability and low-cost preparation with various techniques. All the aforementioned properties of carbon dots make them promising candidates to be used as light absorbance materials.[9] However, the use of carbon dots or nitrogen doped materials solely as light harvesters with

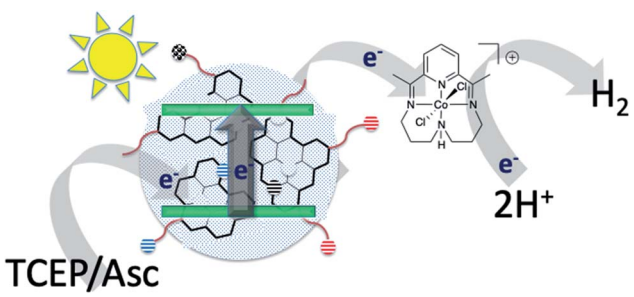

Fig. 1 Schematic representation of photo driven H_2 production with carbon dots as the photosensitizer in the presence of a cobalt catalyst.

Laboratory of Bioinorganic Chemistry, Chemistry Department, University of Crete, 70013 Heraklion, Crete, Greece. E-mail: kladomenou@uoc.gr; gcharal@uoc.gr; acoutsol@uoc.gr

† Electronic supplementary information (ESI) available. See DOI: 10.1039/d0se01630f

molecular catalysts is limited.[15,16] In contrast there are reports of their use as photosensitizers through co-sensitization with TiO_2 and in the presence of noble metal catalysts.[17–19] Therefore, there is a need to develop an efficient system comprised of carbon dot materials with noble metal free molecular catalysts.

In this report carbon dots (**CDot**) and N-doped carbon dots (**NCDot**) have been synthesized as light harvesters to direct photocatalysis of protons to H_2 with the use of molecular cobalt catalysts (Fig. 1). The molecular H_2 evolving catalysts that were selected herein are cobalt based, the macrocyclic **CatCo(III)1**, the cobaloxime **CatCo(III)2**, and the porphyrin based catalyst **CatCo(II)3** (Fig. 6). This molecular approach regarding the catalysts presents the advantage of facile synthetic preparation and future modification of the compounds, in order to investigate a series of molecules. The carbon dot materials were efficiently synthesized and physically and structurally characterized. Additional studies were performed concerning UV-vis, fluorescence properties and electron transfer capability of all carbon dot materials. H_2 photocatalytic experiments exhibited a high production rate of 859 TON_{CAT} with **NCDot** as the light harvesting material and **CatCo(III)1** as the molecular catalyst in the presence of a SED. This value is the highest reported in the literature concerning analogue Co based systems.[20] The main drawback of this photocatalytic scheme is the use of the SED that inhibits it from being a real sustainable system for H_2 evolution. Nevertheless, these materials present a remarkable stability during photocatalysis that makes them able to produce H_2 even after a period of 3 weeks under real solar irradiation, the Cretan sunlight. Also, a H_2 evolution mechanism of our best working system is proposed.

Results and discussion

Synthesis of carbon dots

Various water-soluble carbon dots were synthesized as photosensitizers for efficient hydrogen production using molecular cobalt based catalysts. Bottom-up synthesis was used for the preparation of the carbon dots starting from inexpensive organic materials that were thermally decomposed to form the appropriate carbon core. In this work two different types of materials were prepared **CDot** and **NCDot**. The first is designed with sodium carboxylate groups, while the second is doped with nitrogen and contains carboxylic acid and amino terminated groups. In both types of carbon dots citric acid was used as a carbon source. In the case of **CDot** citric acid was pyrolyzed to form carboxylic acid terminated carbon dots followed by neutralization with NaOH. More specifically, an already published synthetic procedure was followed with slight modification.[21] Powder citric acid was heated in an oven under air at 180 °C for 72 h to obtain a brown powder as shown in Scheme 1.

For the preparation of **NCDots**, citric acid was hydrothermally treated in the presence of ethylenediamine (Scheme 1).[22,23] Citric acid was dissolved in water in a poly(tetrafluoroethylene)-lined autoclave reactor and heated at 180 °C for 8 h. The dark brown products were added in a dialysis membrane bag 1 kDa for 24 h in order to remove residual citric acid and small sized products. The product was added in a round-bottomed flask and freeze-dried in order to obtain **NCDot** as a dark powder (Scheme 1). Also, **NCDotMix** was obtained following the same procedure by skipping the step of purification; therefore, the reaction mixture was collected from the reactor and freeze-dried to obtain a brown solid. The yield of all the above synthetic procedures was about 35–40%. The nature and the properties of the synthesized material were studied with several spectroscopic techniques.

Physical characterization of carbon dots

FT-IR spectroscopy was performed in order to obtain information about the surface functionalities of carbon dots. The **CDot** spectrum (Fig. 2) shows a broad peak in the range of 3335–2900 cm^{-1} that corresponds to vibration of N–H, O–H, and C–H bonds and peaks at 1560 and 1387 cm^{-1} that correspond to antisymmetric and symmetric stretches of the carboxylate group, as already referred to in the literature.[24] The spectrum of **NCDot** displays the following peaks: 3241 cm^{-1} that corresponds to N–H and O–H vibrations, 2920 cm^{-1} (C–H), 1684 cm^{-1} (C=C), 1646 cm^{-1} (C=O), and 1531 cm^{-1} (N–H). In the FT-IR spectrum of both materials the C=O vibration of citric acid at 1742 cm^{-1} (C=O) is not present, therefore the shift and the broadness of the peaks imply full carbonization of both carbon dot materials of both **CDot** and **NCDot**.

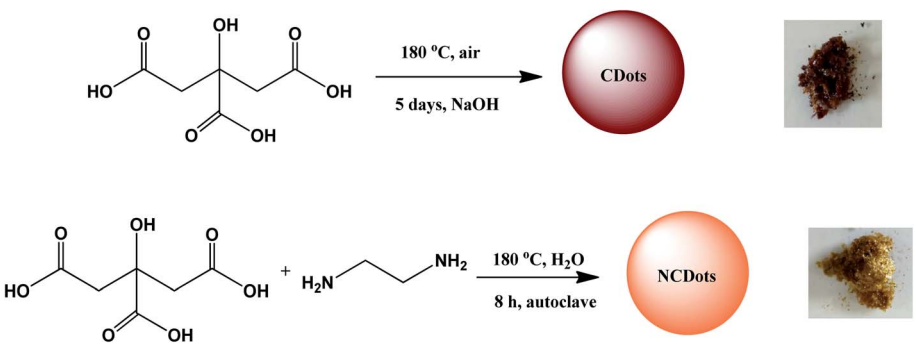

Scheme 1 Synthetic procedure for the preparation of carbon dots **CDots** and **NCDots**.

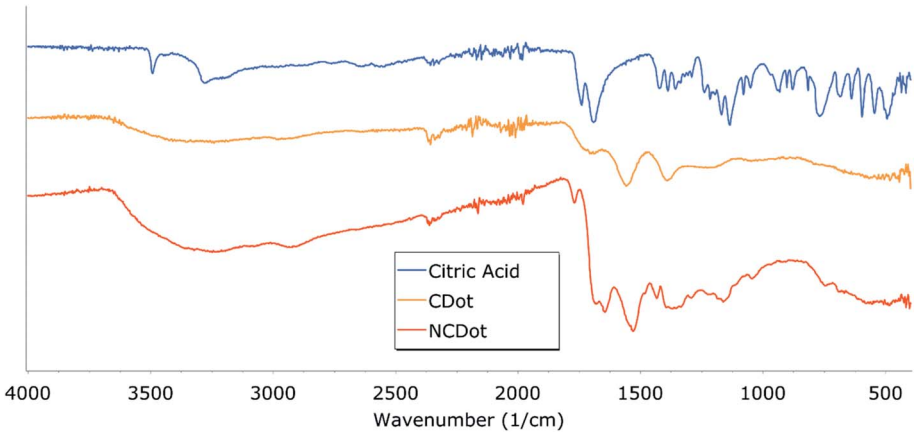

Fig. 2 FT-IR spectra of citric acid, **CDot** and **NCDot**.

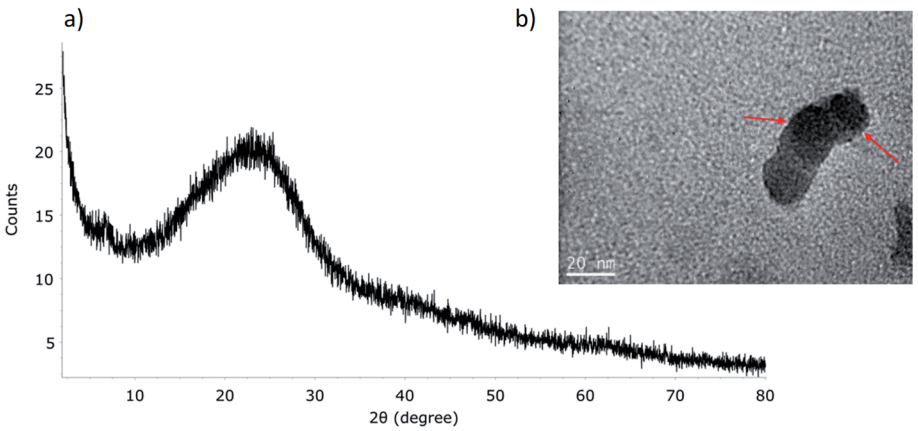

Fig. 3 (a) XRD pattern and (b) TEM image of **NCDots**.

Structural information

The morphology of carbon dots was observed by transmission electron microscopy TEM as shown in Fig. 3b and S1b.† The **CDot** nanoparticles show a near spherical morphology with a diameter of about 50 nm (Fig. S1b†) where in the case of **NCDot** the diameter of the material is less than 20 nm (Fig. 3b). In order to further elucidate the structure of carbon dots X-ray powder diffraction (XRD) was performed. **NCDot** displayed a broad peak at $2\theta = 23^{\circ}$, which is attributed to highly defected or disordered carbon atoms as shown in Fig. 3a. The broad peak is a characteristic peak of the long-range disorder structure due to the small size of **NCDot** as shown in TEM images (Fig. 3b).[25] In the case of **CDot** an amorphous peak at $2\theta = 30^{\circ}$ was observed in the XRD measurements (Fig. S1a†).

UV-vis and fluorescence

The aqueous solutions of carbon dots in all cases were yellow under daylight. All materials emitted blue fluorescence under 360 nm UV lamp radiation. The UV-vis spectrum of **CDot** in H_2O (Fig. 4a) showed an absorption at *ca.* 200 nm, a typical absorption peak which is assigned to the $\pi \rightarrow \pi^*$ transition of the aromatic sp^2 areas.[26] **NCDot** showed two peaks one at *ca.* 200 nm and an absorption peak at 340 nm (Fig. 4b). The first peak can be ascribed to the $\pi \rightarrow \pi^*$ transition of the unsaturated conjugated nanocarbon structure and the latter is due to the $n \rightarrow \pi^*$ transition of the C=O bond.[27] The UV-vis spectrum of **NCDotMix** is similar to **NCDot** and is illustrated in Fig. S2b.† The high energy transition of all carbon dots is due to charge transfer from the inner to outer part of the sp^2-hybridized core. In addition the lower energy transition is related to the transition from the edge or from the surface groups into the core.[28]

In the fluorescence spectra, **CDot** displayed a maximum emission at 360 nm, while **NCDot** and **NCDotMix** showed a maximum emission at 340 nm as shown in Fig. 4 and S2.† The emission of all carbon dots progressively red shift to a longer wavelength as the excitation increases beyond 320 nm showing an excitation-dependent behavior that is well known in similar carbon dot materials.[29]

Quantum yield and lifetime

The quantum yield (QY) of carbon dots was calculated using quinine hemisulfate in 0.1 M H_2SO_4 as a reference. The QY of **NCDot** was calculated to be 26%, whereas for **CDot** a much

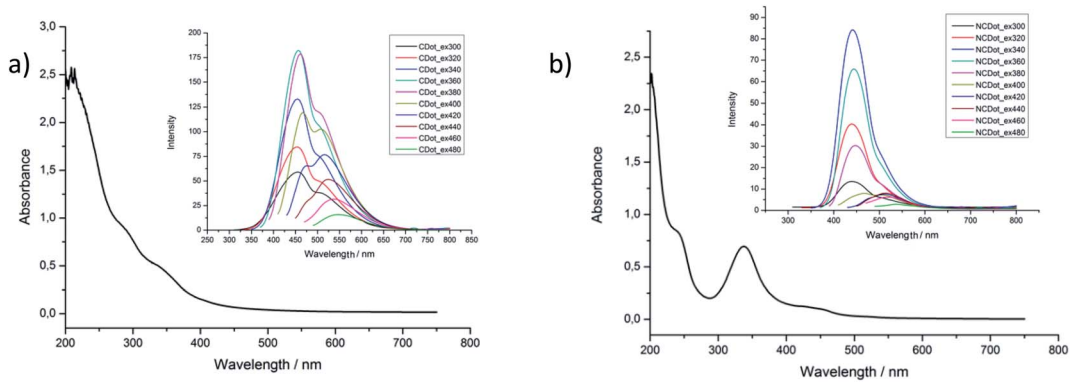

Fig. 4 UV-vis absorption and fluorescence spectra of (a) **CDot** and (b) **NCDot**.

lower QY of 2% was measured indicating that N doping is an effective method to enhance the photoluminescence of these materials.[30] Moreover, the QY of **NCDotMix**, which is the material obtained directly from the reaction with no further purification, was calculated to be 43%. This indicates that the carbon dots with a small molecular weight appear to have larger QY. Lifetime decay fluorescence measurements of **NCDot** showed $\tau_1 = 3.7$ (38%) ns and $\tau_2 = 14.7$ (62%) ns whereas the **CDot** showed $\tau_1 = 2.1$ (76%) ns and $\tau_2 = 14.4$ (24%) ns. The values were calculated by using a double-exponential function for the satisfactory data fitting. These measurements are according to the literature since it is known that carbon dot materials show multiexponential decay of photoluminescence emission.[31]

Table 1 Valence band (VB) and conduction band (CB) potentials and optical band gap (E_{00}) of all carbon dots

Carbon dots	E_{VB} [a] (V)	E_{CB} [b] (V)	E_{00} [c] (eV)
NCDot	+1.01	−2.13	3.14
NCDotMix	+1.01	−2.13	3.14
CDot	+1.18	−1.98	3.16

[a] Oxidation potentials were measured by cyclic voltammetry and were referenced to NHE by addition of +0.193 V.[33] [b] Values were calculated as the difference of the oxidation potentials and the optical band gap energy E_{00}, calculated in eV. [c] E_{00} values were calculated from the intersection between the normalized absorption and emission spectra.

Electron transfer assays

The electron transfer ability of carbon dots was investigated by observing the photoreduction of methyl viologen (MV^{2+}) and its capability to quench photoluminescence.[24] Therefore, a solution of MV^{2+} in aqueous ethylenediaminetetraacetic acid (EDTA), at pH = 6 and in the presence of **NCDot** was bubbled for 15 min under argon in order to remove oxygen. After 2 min of UV irradiation the typical peaks of reduced methyl viologen ($MV^{+\cdot}$) at 395 and 603 nm appeared as shown in Fig. 5a. During the time, the color of the solution changed from yellow to blue that is indicative of the formation of the reduced species. The same experiments were performed with **CDot** displaying the same spectra (Fig. 5b). Therefore, the carbon dots have electron transfer properties which are essential for the photocatalysis.

Electrochemical measurements

Cyclic voltamograms of all materials (Fig. S3–S5†) were obtained in 0.1 M aqueous solution of sodium sulfate. The oxidation and reduction potentials are presented in the ESI (Table S1).† The oxidation potentials of carbon dots were used as the valence band (VB) values of the photosensitizers, since it has been reported in the literature that for similar systems such as CdTe quantum dots the E_{ox} provides estimated values of the position of the VB.[32] Then, the VB values were subtracted from the optical energy values (E_{00}) in order to obtain the potentials of the conduction band (CB). The E_{00} values were obtained from

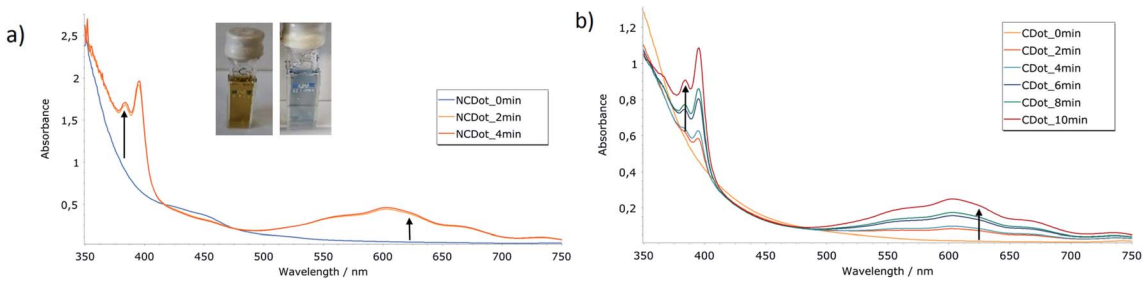

Fig. 5 UV-vis spectra of (a) **NCDot** (0.5 mg ml^{-1}) with methyl viologen (1.2 mM) in EDTA 0.1 M at pH = 6 and (b) **CDot** (0.5 mg ml^{-1}). UV-vis spectra were recorded every 2 min after irradiation with a UV lamp.

the intersection between the normalized absorption and emission spectra of carbon dots. In the case of **NCDot** E_{00} was estimated at 395 nm that correspond to 3.14 eV. All calculated values are listed in Table 1 and the normalized spectra of **CDot** and **NCDot** are shown in Fig. S9 and S10,† respectively.

Synthesis of catalysts

Cobalt based water-soluble molecular catalysts **CatCo(III)1**, **CatCo(III)2** and **CatCo(II)3** were used for our H_2 evolution experiments (Fig. 6). The first Co catalyst (**CatCo(III)1**) was synthesized according to the synthetic procedure described by Busch and later modified by Collomb and coworkers.[34,35] The last step of the aforementioned procedure was the treatment of 2,6-diacetylpyridine with $CoCl_2 \cdot 6H_2O$ salt, diaminodipropylamine and $LiClO_4$ to afford the desired product in good yield. Then the second cobaloxime based catalyst **CatCo(II)2** was prepared from dimethylglyoxime $[Co(dmg)_2Cl_2]$ with the addition of L-histidine under a N_2 atmosphere.[36,37] A water-soluble cationic Co-porphyrin catalyst **CatCo(II)3** was synthesized as described previously by metalation of tetrapyridylporphyrin with $(CH_3COO)_2Co \cdot 4H_2O$ in DMF under reflux. Finally, methylation was achieved by adding excess of iodomethane.[38]

Photocatalytic hydrogen production

Photocatalytic experiments were performed using carbon dots as photosensitizers and different cobalt molecules as catalysts (Fig. 6) in aqueous solution with the use of diverse sacrificial electron donors (SEDs) as shown in Fig. 1. In our first attempts the catalytic system comprised of **CDot** and N-doped carbon dots pure (**NCDot**) and impure (**NCDotMix**) as photosensitizers with **CatCo(III)1** in 0.1 M or 1 M ascorbic acid (Asc) as the SED at pH = 5. The system was irradiated under UV or visible white LED light and in any case no H_2 was detected. This may be attributed to the well-known formation of dehydroascorbic acid (DHA), which is produced during the catalysis and prevents the ability of Asc to provide electrons to the photosensitizer.[39] To overcome this difficulty we used SED as a mixture of TCEP/Asc (1 : 1) 0.1 M each at pH = 5 and H_2 was produced in all cases in the presence of **CatCo(III)1** as a molecular catalyst. The same SED mixture had been previously used by us and others leading to a more efficient hydrogen evolution in all systems.[20,40,41] TCEP regenerates the oxidized ascorbic acid and therefore overcomes the limitation of instability of Asc and extends the lifetime of the system. Upon optimization of the system the maximum TON_{CAT} of 859 was reached when N-doped carbon dots (**NCDot**) were used as the photosensitizer after 52 h of irradiation (Fig. 7). This is the highest TON_{CAT} reported in the literature when carbon dots are used as a photocatalyst with a cobalt molecule as a catalyst. The **CatCo(III)1** catalyst was chosen since it shows great stability and activity for H_2 evolution in aqueous media.[35,42] Moreover it has been used previously in a system of CdTe water soluble quantum dots and reached 650 TON_{CAT} in 1.5 h where it is less efficient compared to our system indicating that for a better performance, CdTe components are not essential. Also, our photosensitizers are easily synthesized from low-cost starting materials.[43]

In the case of impure carbon dots (**NCDotMix**) the maximum TON_{CAT} 334 was attained at 23 h, whereas the maximum TON_{CAT} of **CDot** was 64 at 23 h. The lower performance of **NCDotMix** compared to that of the pure ones is possibly due to the presence of citric acid or due to carbonated products with low molecular weight that prevent the absorption of light from the photosensitizer. A characteristic feature of N-doped carbon dots is that they start producing H_2 after about 10 h of irradiation at a slower rate compared to **CDot**. More specifically, after 7 h of irradiation no H_2 was detected for **NCDot** and **NCDotMix**, while at 7 h **CDot** attained 52 TON_{CAT}. Therefore, in our system the **NCDot** chromophore proved to be more efficient compared to **CDot**. The enhanced TON measured for N-doped carbon dots is well known in the literature, since the presence of nitrogen improves the charge transfer by introducing n-domains in the material.[13,44]

In all cases the system is stable after UV irradiation for about 6 days. Reisner and co-workers have already reported H_2 evolution of carbon dots using water-soluble cobalt catalysts and carboxylate terminated carbon dots, under similar conditions.[20] They observed a low rate of H_2 production TON_{CAT} ranging from 141 to 56 and a high stability of their system, being active after 4 days of irradiation. In the case of N-doped carbon dots the performance of our catalyst was much better compared to all molecular cobalt catalysts reported in the literature.[20] To the best of our knowledge our system shows the highest rates of H_2 production when N-doped carbon dots are

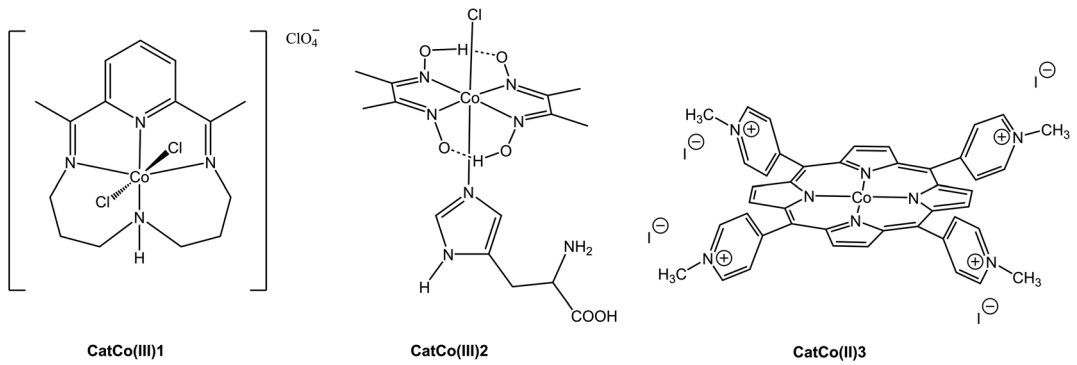

CatCo(III)1 CatCo(III)2 CatCo(II)3

Fig. 6 Molecular structures of cobalt catalysts used in this work for H_2 production.

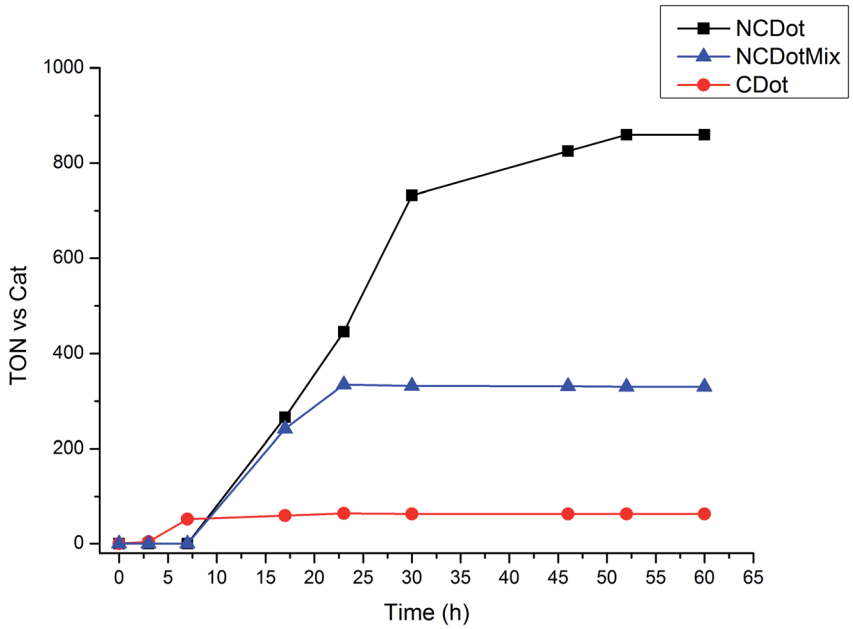

Fig. 7 Photocatalytic hydrogen production plots of **NCDot**, **NCDotMix** and **CDot**. The photocatalytic experiments were conducted in aqueous TCEP/Asc (1 : 1) 0.1 M each at pH = 5. The amount of carbon dots was 10 mg in each case and the catalyst **CatCo(III)1** (20 nmol). All the results presented in the H_2 production plots are the average values of three independent measurements (within 5–10% error).

photosensitized in the presence of a cobalt molecular catalyst in water. Our system proved to be very stable since after about 6 days the carbon dots started to photo bleach and the system stopped producing more H_2. The photo bleaching of the photosensitizer was monitored with UV-vis spectroscopy (Fig. S6†). As shown in the spectra the absorption of the material is decreasing overtime indicating the decolorization of the material upon UV irradiation. Therefore, after about 70 h of irradiation the system was not able to absorb more light and the H_2 production stopped. In order to investigate further the state of carbon dots during and after the photocatalytic experiment TEM images were obtained in order to investigate if there is a change in the morphology of carbon dots (Fig. S7†). In Fig. S7(a)† the spheres of **NCDot** are shown after UV irradiation for 50 h and in Fig. S7(b)† are presented in the **NCDot** after the completion of the photocatalytic experiment. It is evident that the carbon dot materials keep their spherical shape but their diameter gets smaller upon light irradiation. Moreover, the number of the spheres is less upon irradiation. Consequently, it seems that upon irradiation the morphology of the photosensitizer alters. This is in accordance with XRD measurements that were done in **NCDot** after the photocatalytic experiment (Fig. S8†). The broad peak that was present at $2\theta = 23^\circ$ is the starting material, after 70 h of irradiation the same peak was diminished indicating that the structure of the material has been changed.

Moreover, control experiments were performed in the absence of the catalyst **CatCo(III)1**, in the absence of the photosensitizer **NCDot**, in the absence of the SED, TCEP/Asc and in the dark. In any case a negligible amount of H_2 was produced. This indicates that all components are essential for H_2 production in our system. Also, when 20 nmol of $CoCl_2$ was used as an alternative of the Co molecular catalyst, insignificant H_2 was evolved. In addition, control H_2 evolution experiments were done using **NCDot**, **CatCo(III)1** and TCEP as the SED (0.1 M at pH 5), where a lower photocatalytic H_2 production of 462 TON_{CAT} was observed. This revealed that even though **NCDot** can oxidize the TCEP, the Asc is the one that quenches the photoinduced holes and the combination of TCEP/Asc is essential for efficient H_2 production.[20] This finding is in accordance with the emission experiments of **NCDot** where in the

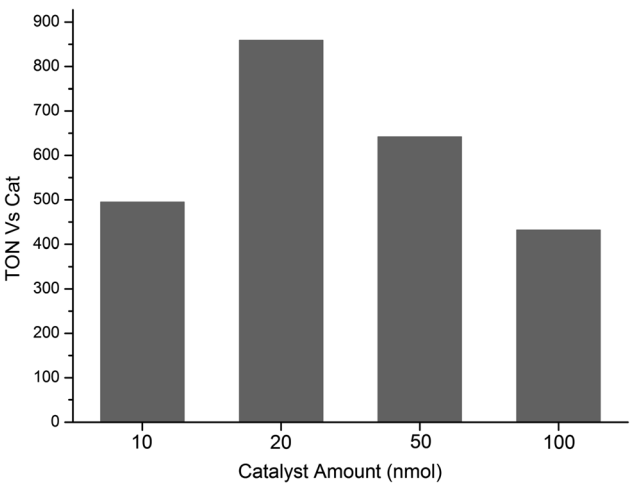

Fig. 8 Photocatalytic hydrogen production plots **NCDot** in four different quantities of the catalyst **CatCo(III)1**: 10, 20, 50 and 100 nmol. The photocatalytic experiments were conducted in aqueous TCEP/Asc (1 : 1) 0.1 M each at pH = 5 in the presence of catalyst **CatCo(III)1**. All the results presented in the H_2 production plots are the average values of three independent measurements (within 5–10% error).

presence of 0.1 M TCEP the carbon dots were slightly quenched (Fig. S11†).

Subsequently, the quantity of the catalyst was evaluated by using four different amounts 10, 20, 50 and 100 nmol of **CatCo(III)1** in aqueous solution of TCEP/Asc 0.1 M each (Fig. 8). The maximum TON_{CAT} was obtained when 20 nmol of **CatCo(III)1** was used, therefore all the photocatalytic experiments that are reported herein were done with 20 nmol of catalyst.

In our attempt to find out if our photosensitizer works well with other water soluble catalysts we performed catalytic experiments using **NCDot** as the photosensitizer and **CatCo(III)2** and **CatCo(II)3** as catalysts (Fig. 9). The thermodynamics of the system using these two molecules makes them promising catalysts for H_2 production.[11,45] In our first attempt, when 20 nmol of the cobaloxime-type catalyst **CatCo(III)2** was used for H_2 evolution experiments 1.01 μmol H_2 was obtained after 46 h of UV irradiation. Moreover, when 20 nmol of water-soluble cobalt porphyrin **CatCo(II)3** was the catalyst, no H_2 was detected after 74 h of UV irradiation. The maximum amount of H_2 17.1 μmol was obtained with the stable **CatCo(III)1** after 52 h of light irradiation making this Co catalyst superior compared to the other two catalysts. The small H_2 production of **CatCo(III)2** can be due to its low stability in acidic aqueous media already reported in the literature.[43] In addition the undetectable H_2 in the case of **CatCo(II)3** is possibly once again due to the low stability of the porphyrin molecule under UV irradiation.[46]

In order to understand better the high performance of **CatCo(III)1** the ΔG (PS/Cat) were calculated for the three catalysts and the photosensitizer **NCDot**. The redox potentials of the reported compounds and the thermodynamic driving forces for the electron transfer process are listed in Table 2. The thermodynamic driving forces were calculated according to the literature.[47] From these results it is obvious that the driving force of **CatCo(III)1** is larger compared to the other two catalysts which is in accordance with the grater H_2 production of this catalyst.

Table 2 Redox potentials (V *vs.* NHE) of the photosensitizer and catalysts with the thermodynamic driving forces of electron transfer processes ΔG_1 (PS/Cat) and ΔG_2 (PS/Cat) (eV)

Compounds	$E_{1/2}$ Ox			$E_{1/2}$ Red
NCDot	+1.01			−0.87
	$E_{1/2}$ $Co^{III/II}$	$E_{1/2}$ $Co^{II/I}$	ΔG_1 (PS/Cat)	ΔG_2 (PS/Cat)
CatCo(III)1 (ref. 43)	+0.35	−0.61	−1.22	−0.26
CatCo(III)2 (ref. 37)	−0.48	−0.87	−0.39	0
CatCo(II)3 (ref. 48)	−0.26	−0.46	−0.61	−0.41

In all the catalytic systems H_2 evolution reaches a plateau after several hours of irradiation and the H_2 production stops. After the addition of either the catalyst or the SED no hydrogen production was observed. However, when the photosensitizer, **NCDot** was added, the catalytic system was effectively regenerated, suggesting that the carbon dots are decomposed after about 6 days of UV light irradiation.

Different irradiation sources were applied to broaden the use of our best performing system as shown in Fig. 10. Visible led light was used to obtain 11.6 μmol in 46 h, slightly less compared to the H_2 evolution with UV irradiation (17.1 μmol) possibly due to the higher absorbance of the photosensitizer **NCDot** at the UV region as shown in the UV-vis spectrum Fig. 4b. Finally, we performed the same experiment under the Cretan sun. During 21 days of irradiation the **NCDot** remained stable with no observed photo bleaching, making the system very promising for future use obtaining 5.3 μmol of H_2 (TON_{CAT} = 264).

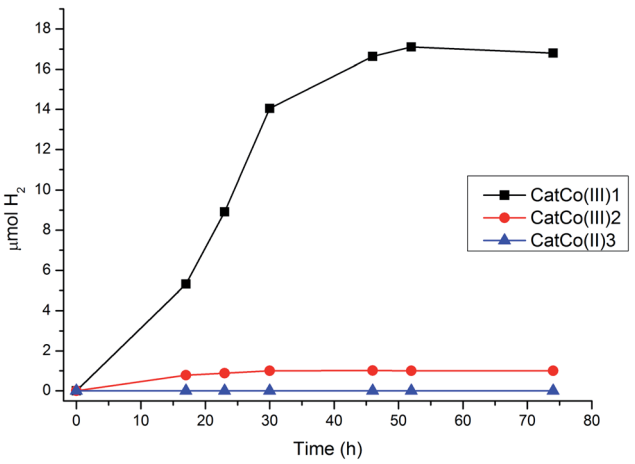

Fig. 9 Photocatalytic hydrogen production plots of 10 mg **NCDot** with catalysts: **CatCo(III)1** (20 nmol), **CatCo(III)2** (20 nmol) and **CatCo(II)3** (20 nmol). The photocatalytic experiments were conducted in aqueous TCEP/Asc (1 : 1) 0.1 M each at pH = 5. All the results presented in the H_2 production plots are the average values of three independent measurements (within 5–10% error).

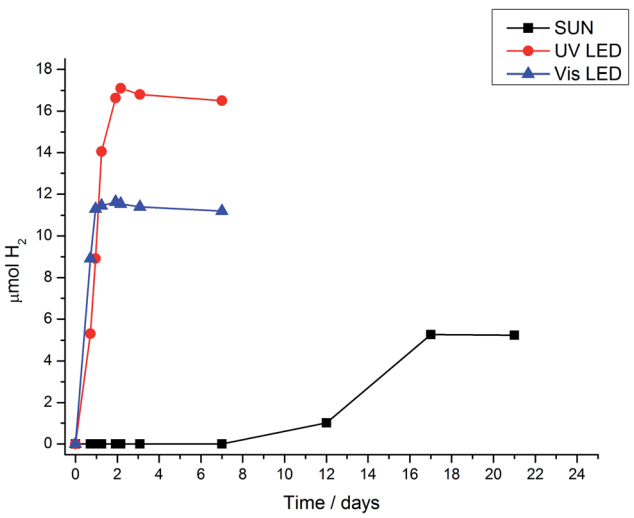

Fig. 10 Photocatalytic hydrogen production plots of 10 mg **NCDot** with **CatCo(III)1** (20 nmol) in various solar sources: UV Vis led and Cretan sun. The photocatalytic experiments were conducted in aqueous TCEP/Asc (1 : 1) 0.1 M each at pH = 5. All the results presented in the H_2 production plots are the average values of three independent measurements (within 5–10% error).

H_2 evolution mechanism

In order to clarify the mechanism of our photocatalytic system we performed emission spectroscopy experiments of **NCDot** in the presence of different concentrations of the cobalt catalyst, **CatCo(III)1**. This experiment will help us understand the favorable pathway that occurs in our system: (a) an oxidative quenching from the chromophore to the catalyst or (b) a reductive quenching from the SED to the chromophore.[6,49] The **NCDot** was excited at 340 nm and upon addition of the catalyst the emission intensity was decreased by about 50% indicating efficient transfer from the CB of the material to the cobalt catalyst (Fig. S12†). The concentration of **NCDot** was kept constant during the addition of the catalyst. An analogous procedure was followed using an aqueous solution of **NCDot** at the same concentration as in the previous experiment and we monitored the emission upon excitation at 340 nm when different concentrations of ascorbic acid at pH = 5 were added (Fig. S13†). Once again, the emission intensity was significantly decreased by about 80%. The mixture of TCEP/Asc was not examined since when 0.1 M concentration of TCEP was used, we observed a slight quenching (Fig. S11†). Therefore, the quenching was due to the presence of the ascorbic acid in the solution. Subsequently, the Stern–Volmer constant K_{sv} was calculated to understand better the mechanism of the photocatalytic reaction. The calculation was done from the fitting of the experimental data according to equation $I_o/I = 1 + K_{SV}[Q]$, where I_o and I are the fluorescence intensities observed in the absence and in the presence of each quencher, respectively, and [Q] is defined as the quencher concentration (Fig. S14†).[50] The K_{SV} in the case of the catalyst was bigger ($K_{SV(cat)} = 4612.8\ M^{-1}$) compared to the sacrificial electron donor ascorbic acid ($K_{SV(Asc)} = 13.8\ M^{-1}$). Moreover, the quenching constant K_Q was calculated using $K_{SV} = K_Q\tau$, where τ stands for the excited state lifetime in the absence of the quencher. In the case of the catalyst **CatCo(III)1** the $K_{Q(cat)} = 4.38 \times 10^{11}\ M^{-1}\ s^{-1}$ and in the case of the sacrificial agent ascorbic acid $K_{Q(Asc)} = 1.32 \times 10^{9}\ M^{-1}\ s^{-1}$. Under similar conditions to the photocatalytic H_2 experiments 6 μM of catalyst and 0.1 M of the SED, the quenching is more prominent in the case of ascorbic acid. This finding suggests that a photoinduced electron transfer takes place from the sacrificial electron donor to the VB of carbon dots. Moreover, even though the quenching constant of the catalyst is greater compared to the ascorbic acid the main electron transfer follows the pathway from the ascorbic acid to the CB of carbon dots due to the greater concentration of the SED (0.1 M) compared to the catalyst (0.6×10^{-5} M).[51] Therefore, the hydrogen production in our system is done through a reductive quenching by using the SED, leading over the oxidative quenching by the **CatCo(III)1**.

The photocatalytic H_2 production seems to be thermodynamically feasible and the energy diagram of the whole process is shown in Fig. 11. The VB and CB potentials of **NCDot** were calculated and are shown in Table 1, whereas the potentials of the SED ascorbic acid and the catalyst **CatCo(III)1** were taken from the literature.[43,52] The photo driven mechanism of H_2 evolution that is proposed herein is in accordance with the mechanism already mentioned by Llobet and Palomares in a similar system using the same cobalt catalyst.[43] In the beginning of the photocatalytic experiment **CatCo(III)1** is in the reduced form Co(II), as observed by the UV-vis spectra, where the addition of the SED reduces the catalyst (Fig. S15†). However, the oxidized form of the catalyst Co(III) can be

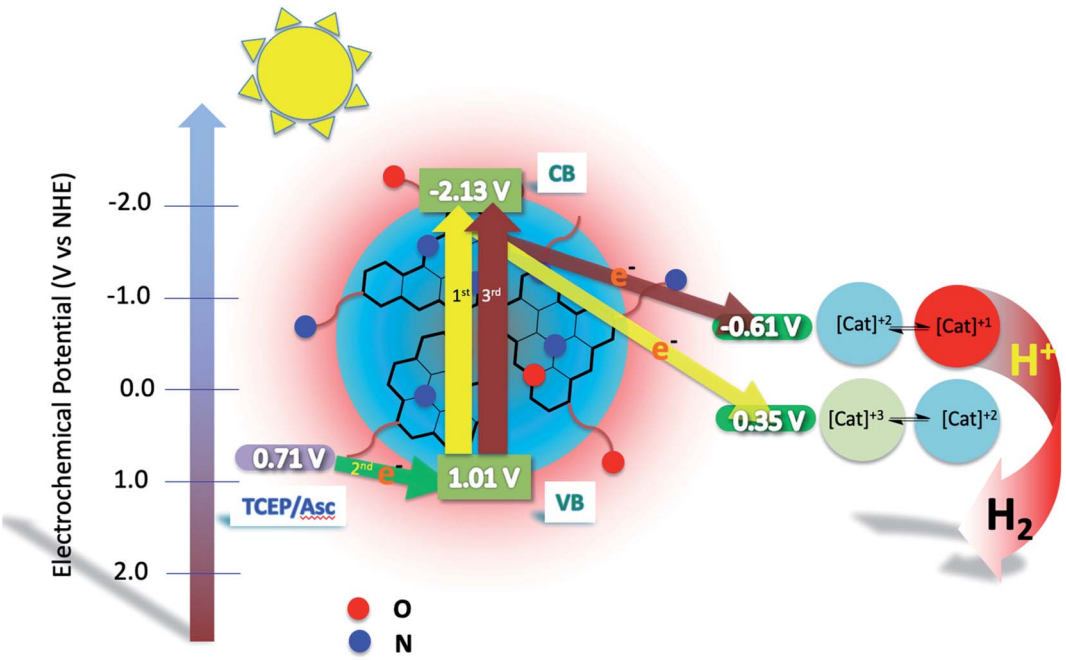

Fig. 11 Mechanism of two electron transfer photocatalytic H_2 production using N-doped carbon dots, **CatCo(III)1** as the catalyst and TCEP/Asc (1 : 1) 0.1 M each as the SED.

produced during H_2 production. In order to produce H_2 two electrons are needed to be transferred to the protons. In our system solar irradiation excites the carbon dots and electron transfer occurs from the VB to the CB, then the hole that is formed at the VB of the photosensitizer is filled with an electron transferred from the sacrificial electron donor. This pathway is in accordance with the reductive quenching of our system as discussed previously.

Following this, one electron reduces the cobalt metal of the catalyst from Co(III) to Co(II). The whole process takes place one more time where a second electron reduces the catalyst. According to theoretical calculations from Zhong, Lu, Sakai and co-workers this second reduction is ligand based and not metal-centered.[53] Therefore, ligand-reduced species formulated as $[Co^{II}(L^{-\bullet})]^+$ are formed, where after their protonation solar H_2 evolution is achieved.

Conclusions

In this work we have examined the H_2 evolution ability of carbon dots and nitrogen doped materials, in the presence of cobalt catalysts in aqueous media. The key substance for efficient H_2 production was TCEP/Asc which acts as the sacrificial electron donor material. TCEP is well known to prevent the formation of dehydroascorbic acid that prevents the ability of ascorbic acid to give electrons to the photosensitizer. The study demonstrated that cobaloxime and porphyrin based cobalt catalysts are not able to promote the photocatalysis. However the quite stable cyclic catalyst **CatCo(III)1** was capable of producing a record high H_2 production of 17.1 μmol (TON_{CAT} = 859) under UV radiation. The photocatalytic H_2 production of our system is performed *via* a reductive quenching by the SED whereas two electrons are needed to be transferred to the protons for H_2 production. This system offers great potential for future work, to explore more water-soluble catalysts and even extend the doping onto the carbon dots with noble-metal free elements in order to improve the light absorption ability. The only drawback of this system is the use of a SED. The improved photocatalytic system can be even applied in the real world since the sun is able to produce H_2 and by just adding low-cost carbon dots onto the system it can operate for several weeks.

Conflicts of interest

There are no conflicts to declare.

Acknowledgements

This research was funded by the General Secretariat for Research and Technology (GSRT) and Hellenic Foundation for Research and Innovation (HFRI; project code: 508). This research has been co-financed by the European Union and Greek National Funds through the Regional Operational Program "Crete 2014-2020", project code OPS: 5029187. In addition the research has been funded by IKY scholarships through the Operational Program "Human Resources Development, Education and Lifelong Learning 2014–2020", Act: "Strengthening of human research potential through the implementation of doctoral research" – MIS 5000432. Moreover, the European Commission's Seventh Framework Program (FP7/2007-2013) under grant agreement no. 229927 (FP7-REGPOT-2008-1, Project BIO-SOLENUTI) and the Special Research Account of the University of Crete are gratefully acknowledged for the financial support of this research.

References

1 M. Pagliaro, A. G. Konstandopoulos, R. Ciriminna and G. Palmisano, *Energy Environ. Sci.*, 2010, **3**, 279–287.
2 K. S. Joya, Y. F. Joya, K. Ocakoglu and R. van de Krol, *Angew. Chem., Int. Ed.*, 2013, **52**, 10426–10437.
3 J. H. Kim, D. Hansora, P. Sharma, J.-W. Jang and J. S. Lee, *Chem. Soc. Rev.*, 2019, **48**, 1908–1971.
4 S. Chu and A. Majumdar, *Nature*, 2012, **488**, 294–303.
5 A. J. Esswein and D. G. Nocera, *Chem. Rev.*, 2007, **107**, 4022–4047.
6 K. Ladomenou, M. Natali, E. Iengo, G. Charalampidis, F. Scandola and A. G. Coutsolelos, *Coord. Chem. Rev.*, 2015, **304**, 38–54.
7 T. S. Teets and D. G. Nocera, *Chem. Commun.*, 2011, **47**, 9268–9274.
8 J. Gao, M. Zhu, H. Huang, Y. Liu and Z. Kang, *Inorg. Chem. Front.*, 2017, **4**, 1963–1986.
9 G. A. M. Hutton, B. C. M. Martindale and E. Reisner, *Chem. Soc. Rev.*, 2017, **46**, 6111–6123.
10 M. Wang, K. Han, S. Zhang and L. Sun, *Coord. Chem. Rev.*, 2015, **287**, 1–14.
11 D. Dolui, S. Ghorai and A. Dutta, *Coord. Chem. Rev.*, 2020, **416**, 213335.
12 H. Luo, Q. Guo, P. Á. Szilágyi, A. B. Jorge and M.-M. Titirici, *Trends Chem.*, 2020, **2**, 623–637.
13 C. Hu, M. Li, J. Qiu and Y.-P. Sun, *Chem. Soc. Rev.*, 2019, **48**, 2315–2337.
14 M. Han, S. Zhu, S. Lu, Y. Song, T. Feng, S. Tao, J. Liu and B. Yang, *Nano Today*, 2018, **19**, 201–218.
15 S. Cao and J. Yu, *J. Photochem. Photobiol., C*, 2016, **27**, 72–99.
16 Y. Liu, H. Huang, W. Cao, B. Mao, Y. Liu and Z. Kang, *Mater. Chem. Front.*, 2020, **4**, 1586–1613.
17 N. C. T. Martins, J. Ângelo, A. V. Girão, T. Trindade, L. Andrade and A. Mendes, *Appl. Catal., B*, 2016, **193**, 67–74.
18 R. Shi, Z. Li, H. Yu, L. Shang, C. Zhou, G. I. N. Waterhouse, L.-Z. Wu and T. Zhang, *ChemSusChem*, 2017, **10**, 4650–4656.
19 I. Sargin, G. Yanalak, G. Arslan and I. H. Patir, *Int. J. Hydrogen Energy*, 2019, **44**, 21781–21789.
20 B. C. M. Martindale, E. Joliat, C. Bachmann, R. Alberto and E. Reisner, *Angew. Chem., Int. Ed.*, 2016, **55**, 9402–9406.
21 C. X. Guo, D. Zhao, Q. Zhao, P. Wang and X. Lu, *Chem. Commun.*, 2014, **50**, 7318–7321.
22 S. Zhu, Q. Meng, L. Wang, J. Zhang, Y. Song, H. Jin, K. Zhang, H. Sun, H. Wang and B. Yang, *Angew. Chem., Int. Ed.*, 2013, **52**, 3953–3957.
23 J. Schneider, C. J. Reckmeier, Y. Xiong, M. von Seckendorff, A. S. Susha, P. Kasák and A. L. Rogach, *J. Phys. Chem. C*, 2017, **121**, 2014–2022.

24 B. C. M. Martindale, G. A. M. Hutton, C. A. Caputo and E. Reisner, *J. Am. Chem. Soc.*, 2015, **137**, 6018–6025.
25 F.-D. Han, B. Yao and Y.-J. Bai, *J. Phys. Chem. C*, 2011, **115**, 8923–8927.
26 D. Pan, J. Zhang, Z. Li and M. Wu, *Adv. Mater.*, 2010, **22**, 734–738.
27 Z. Liang, L. Zeng, X. Cao, Q. Wang, X. Wang and R. Sun, *J. Mater. Chem. C*, 2014, **2**, 9760–9766.
28 C. J. Reckmeier, Y. Wang, R. Zboril and A. L. Rogach, *J. Phys. Chem. C*, 2016, **120**, 10591–10604.
29 P. G. Luo, S. Sahu, S.-T. Yang, S. K. Sonkar, J. Wang, H. Wang, G. E. LeCroy, L. Cao and Y.-P. Sun, *J. Mater. Chem. B*, 2013, **1**, 2116–2127.
30 P. Yang, J. Zhao, J. Wang, H. Cui, L. Li and Z. Zhu, *ChemPhysChem*, 2015, **16**, 3058–3063.
31 P. M. Gharat, J. M. Chethodil, A. P. Srivastava, P. K. Praseetha, H. Pal and S. Dutta Choudhury, *Photochem. Photobiol. Sci.*, 2019, **18**, 110–119.
32 S. K. Haram, A. Kshirsagar, Y. D. Gujarathi, P. P. Ingole, O. A. Nene, G. B. Markad and S. P. Nanavati, *J. Phys. Chem. C*, 2011, **115**, 6243–6249.
33 C. G. Zoski, *Handbook of Electrochemistry*, Elsevier, Amsterdam, 2007.
34 K. M. Long and D. H. Busch, *J. Coord. Chem.*, 1974, **4**, 113–123.
35 S. Varma, C. E. Castillo, T. Stoll, J. Fortage, A. G. Blackman, F. Molton, A. Deronzier and M.-N. Collomb, *Phys. Chem. Chem. Phys.*, 2013, **15**, 17544–17552.
36 G. N. Schrauzer, G. W. Parshall and E. R. Wonchoba, *Bis(Dimethylglyoximato)Cobalt Complexes: ("Cobaloximes"), Inorganic Syntheses*, John Wiley & Sons, Ltd, 2007, pp. 61−70.
37 D. Dolui, S. Das, J. Bharti, S. Kumar, P. Kumar and A. Dutta, *Cell Reports Physical Science*, 2020, **1**, 100007.
38 D. Skrzypek, I. Madejska and J. Habdas, *Solid State Sci.*, 2007, **9**, 295–302.
39 M. Guttentag, A. Rodenberg, R. Kopelent, B. Probst, C. Buchwalder, M. Brandstätter, P. Hamm and R. Alberto, *Eur. J. Inorg. Chem.*, 2012, 59–64.
40 N. Queyriaux, E. Giannoudis, C. D. Windle, S. Roy, J. Pécaut, A. G. Coutsolelos, V. Artero and M. Chavarot-Kerlidou, *Sustainable Energy Fuels*, 2018, **2**, 553–557.
41 S. Schnidrig, C. Bachmann, P. Müller, N. Weder, B. Spingler, E. Joliat-Wick, M. Mosberger, J. Windisch, R. Alberto and B. Probst, *ChemSusChem*, 2017, **10**, 4570–4580.
42 C. C. L. McCrory, C. Uyeda and J. C. Peters, *J. Am. Chem. Soc.*, 2012, **134**, 3164–3170.
43 C. Gimbert-Suriñach, J. Albero, T. Stoll, J. Fortage, M.-N. Collomb, A. Deronzier, E. Palomares and A. Llobet, *J. Am. Chem. Soc.*, 2014, **136**, 7655–7661.
44 B. C. M. Martindale, G. A. M. Hutton, C. A. Caputo, S. Prantl, R. Godin, J. R. Durrant and E. Reisner, *Angew. Chem., Int. Ed.*, 2017, **56**, 6459–6463.
45 J. Ma, J. Wu, J. Gu, L. Liu, D. Zhang, X. Xu, X. Yang and Z. Tong, *J. Mol. Catal. A: Chem.*, 2012, **357**, 95–100.
46 N. M. Berezina, M. B. Berezin and A. S. Semeikin, *J. Mol. Liq.*, 2019, **290**, 111196.
47 N. Queyriaux, R. A. Wahyuono, J. Fize, C. Gablin, M. Wächtler, E. Martinez, D. Léonard, B. Dietzek, V. Artero and M. Chavarot-Kerlidou, *J. Phys. Chem. C*, 2017, **121**, 5891–5904.
48 S.-M. Chen and S.-W. Chiu, *J. Mol. Catal. A: Chem.*, 2001, **166**, 243–253.
49 W. T. Eckenhoff, W. R. McNamara, P. Du and R. Eisenberg, *Biochim. Biophys. Acta, Bioenerg.*, 2013, **1827**, 958–973.
50 J. Keizer, *J. Am. Chem. Soc.*, 1983, **105**, 1494–1498.
51 S. Panagiotakis, G. Landrou, V. Nikolaou, A. Putri, R. Hardré, J. Massin, G. Charalambidis, A. G. Coutsolelos and M. Orio, *Front. Chem.*, 2019, **7**, 405.
52 E. Benazzi, V. C. Coni, M. Boni, R. Mazzaro, V. Morandi and M. Natali, *Dalton Trans.*, 2020, **49**, 10212–10223.
53 J.-W. Wang, K. Yamauchi, H.-H. Huang, J.-K. Sun, Z.-M. Luo, D.-C. Zhong, T.-B. Lu and K. Sakai, *Angew. Chem., Int. Ed.*, 2019, **58**, 10923–10927.

